

Theoretical Study of Cage Clusters of $Zn_{48}O_{48}$, $Zn_{48}S_{48}$ and $Zn_{48}Se_{48}$

Dipali S Lohagaonkar, Shubhangi Ranaware, Sarika J Sali
Guru Gobind Singh Polytechnic, Nashik, Maharashtra, India

Abstract: In this study, we have modulated $Zn_{48}X_{48}$ clusters (where $X=O, S, Se$) using density functional theory. Initially structural, electric, magnetic and optical properties have been investigated. The study compared with earlier work. We tried to investigate, whether these clusters are suitable as shell material to cover any magnetic iron-oxide material. To study core material which do not affect magnetic property of host material we have chosen ZnO material as a shell material along with ZnS and ZnSe materials. In this study we found that all three cage structures are suitable structures with T_h symmetry. Cage clusters are found diameter in the range of 12.15 Å to 14.76 Å. These clusters are found to be nonmagnetic in nature. Optical properties of these clusters show transparency in visible and ultraviolet region. Hence such cage clusters are suitable to hold magnetic materials inside it so as to form a core-shell clusters..

Keywords: Cage Clusters, nonmagnetic, core-shell clusters.

I. INTRODUCTION

Atomic clusters are small fragments of materials containing between a few and several hundred atoms. The study of physical and chemical properties of atomic clusters is one of the most active frontiers in material science [1, 2]. A systematic study of the structure and properties of clusters composed of a variety of elements bridged many fields of physics, particularly atomic, molecular, nuclear and condensed matter physics. Interest in nanoclusters made of II-VI compound semiconductors has grown spectacularly in recent years for their paramount technological potential owing to their special semiconductor properties, that make these compounds suitable for applications such as photo-voltaic solar cells, optical sensitizers, photocatalysts, quantum devices or nano biomedicine. Moreover, nanoclusters made of these materials can be doped in order to modified their properties at will. In this context, spherical hollow nanoclusters provide the chance for endohedral doping, namely, the dopant is placed inside the cavity of the hollow nanoparticle. For instance, doping these nanoclusters endohedrals with transition-metals leads to nanoclusters that would combine the appropriate optical and magnetic properties as to be used in nanomedicine, not only for improving of diagnosis applications, but also in the development of tailored nanomaterials with therapeutic properties to treat, for example, the hyperthermic tumoral regression [3].

In the last few decades, a considerable effort has been devoted to the synthesis and characterization of Zn-based II-VI semiconductor bulk materials, mostly for their high stability, high quantum yields and low cytotoxicity. Among these zinc oxide (ZnO) and zinc sulphide (ZnS), having wide bandgaps of 3.4 eV and 3.7 eV, respectively, and high exciton binding energies of 60 and 40 meV, play a striking role in the electronics industry [4]. Bulk zinc selenide (ZnSe), with a bandgap of 2.7 eV and an exciton binding energy of 20 meV, is also an important candidate in this series for applications in optoelectronics, spintronics [4]. More recently, ZnX , ($X=O, S, Se$) semiconductor nanomaterials have attracted much attention due to their peculiar size- and shape-dependent properties. Along with the experimental work, a great deal of theoretical effort has been devoted to the modelling of Zn-based II-VI nanostructures. Early computational studies focused on small and medium size $(ZnX)_n$, ($X=O, S, Se$) clusters and on their structural and electronic properties [5,6]. The medium sized clusters have been predicted to adopt hollow spherical and tube-like structures [88] while onion- and bulk-like arrangements have been suggested upon increasing their size.

Semiconducting hybrid materials with improved functionalities such as optical, electric and magnetic properties have been considered as potential candidates for a wide range of applications. In recent years, core-shell structures in which metals form the core and ZnO constitutes the shell have attracted intense interest due to their significantly high

effectiveness in improving the photocatalytic activity and the synergistic effect among components [7]. The core-shell architecture avoids exposing the inner core to the environment and thus maximizes the interaction between the building blocks. Recently, the electronic, magnetic and optical properties of TMn doped (ZnO)₄₈, (TM = Fe, Co and Ni) hetero-nanostructure are investigated using the density functional theory (DFT) [8].

II. COMPUTATIONAL DETAILS

First principles spin polarized calculations based on density functional theory performed in the Vienna ab initio Simulation Package (VASP) [9]. The exchange-correlation potential is treated with the generalized gradient approximation (GGA) methods, as described in projector augmented wave method within the Perdew-Burke-Ernzerhof (PAW-PBE) functional [10, 11, 12]. To reduce the interaction between periodic images, the cluster is placed in a cubic cell with an edge length of 30 Å while performing the calculations. For k-point sampling, we used a Γ point for the geometry optimization in the Brillouin zone. All atoms are fully relaxed and the convergence criteria for energy and maximum force are set to 10⁻⁵ eV and 0.001 eV/Å. Electronic and magnetic properties are discussed with respect to the variations in HOMO-LUMO gap, eigenvalue spectrum, Bader charge transfer [13], charge density and magnetic moments of the shell system.

Frequency dependent complex dielectric function matrix is calculated to understand the optical properties, after determination of electronic ground state of the systems. The dielectric function ($\epsilon(\omega)$) is given by,

$$\epsilon(\omega) = \epsilon_1(\omega) + i\epsilon_2(\omega) \quad (1)$$

The real and imaginary part of the dielectric function of shell obtained using the linear response theory [9]. While calculating optical spectra the total number of states included are three times of occupied states for obtaining a well converged spectrum.

III. RESULT AND DISCUSSION

To optimized the shell cluster Zn₄₈X₄₈, we have considered the double bubble structure of Zn₆₀O₆₀. We have optimized Zn₆₀O₆₀ cluster by removing its core Zn₁₂O₁₂ to form Zn₄₈O₄₈ cluster. The optimized Zn₄₈O₄₈ globular cage like cluster was found similar to the configuration mentioned by Wang et. al. [14]. The optimized globular Zn₄₈O₄₈ cluster with Th symmetry is represented in Figure 3.3. This structure consists with six four membered and forty-four six membered rings similar to earlier studies [14, 15, 16]. We found that, the bond length is ranging between 1.87 Å to 1.95 Å, and the diameter of the Zn₄₈O₄₈ cluster is 12.15 Å. The configuration and bond lengths are similar to earlier studies [14,15]. The stability of the cluster can be determined with the help of binding energy (BE) per atom Eb, it is calculated as,

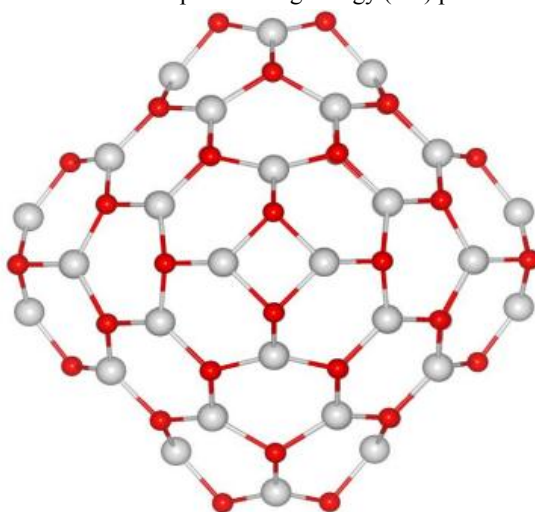


Figure 1.1: Lowest energy configuration of Zn₄₈X₄₈ cluster with X = O, S, Se. Here, Zn atoms are represented by Gray colour and X atoms are represented by red colour, respectively.

$$Eb[Zn_{48}O_{48}] = \frac{-E[Zn_{48}O_{48}] + 48 * E[Zn] + 48 * E[O]}{96} \quad (2)$$

It is found that binding energy of $Zn_{48}O_{48}$ cluster is -3.45 eV/atom. Further, we have studied the electronic properties of $Zn_{48}O_{48}$ cluster. Spin polarized calculations show that cluster is non-magnetic in nature. The nonmagnetic nature of the clusters is also observed through eigenvalue spectrum. Figure 3.4 represents eigenvalue spectra of $Zn_{48}O_{48}$ cluster. The HOMO-LUMO gap of the cluster is found 1.86 eV, which is less than bulk band gap value 3.37 eV [16] as DFT/PBE methods underestimate this gap.

HOMO-LUMO gap for spin up and spin down states is same. The HOMO is triply degenerate in nature. From projected density of states as shown in Figure 3.5, it is observed that upper part of the spectra near HOMO is dominated by O2p states. Middle part of the spectrum is dominated by Zn s, small contribution from Zn d and O p. While lower part of the spectra is dominated by Zn d states. To study nature of bonding in this cluster, we have calculated charge transfer from Zn to O atom using Bader charge analysis [13]. For $Zn_{48}O_{48}$ cluster, average charge on Zn atom is +1.07e and on O atom is -1.07e. This shows ionic nature of Zn-O bond in $Zn_{48}O_{48}$ cluster. As there is significant difference between electronegativity of O (3.44) and Zn (1.65) atoms leads to ionic nature of the cluster.

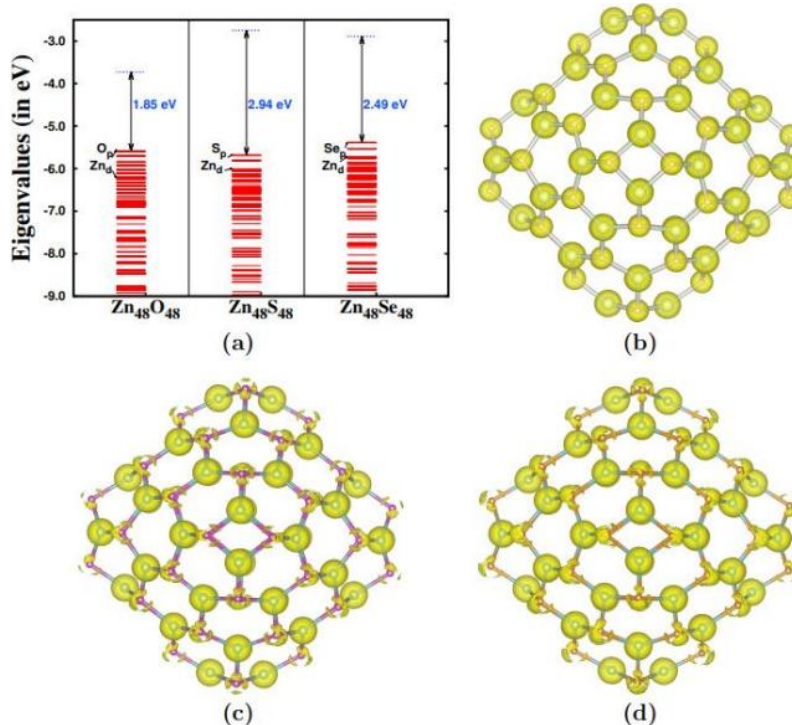


Figure 1.2: (a) Spin up eigen value spectra of $Zn_{48}O_{48}$, $Zn_{48}S_{48}$ and $Zn_{48}Se_{48}$ clusters, here continuous lines represent occupied states and dotted line represents unoccupied state. (b) Total charge density of $Zn_{48}O_{48}$ cluster at the value of $1/7^{th}$ of the maximum total charge density, (c) Charge density of $Zn_{48}S_{48}$ cluster at $1/17^{th}$ of the maximum total charge density and (d) Charge density of $Zn_{48}Se_{48}$ cluster at $1/23^{th}$ of the maximum total charge density.

Here $E[Zn_{48}O_{48}]$ represents the energy of $Zn_{48}O_{48}$ cluster, $E[Zn]$ represents energy of Zn atoms, and $E[X]$ represents energy of X atom, here $X = S$ and Se . It is found that stability of $Zn_{48}O_{48}$ is higher than $Zn_{48}S_{48}$ and $Zn_{48}Se_{48}$, respectively. Binding energy of $Zn_{48}O_{48}$ cluster is -3.45 eV/atom, binding energy of $Zn_{48}S_{48}$ cluster is -2.82 eV/atom and of $Zn_{48}Se_{48}$ cluster is -2.5 eV/atom. Our results are in good agreement with earlier studies [6,15,17]. Further we have studied electronic properties of $Zn_{48}X_{48}$ clusters with the variation in X as O, S and Se, Figure 3.4 represents the eigen value spectrum of $Zn_{48}X_{48}$ system. Due to nonmagnetic nature of these clusters the spin up and spin down nature is almost similar. Hence, we have shown the spin up eigen value spectrum of all the clusters. The eigen value spectrum of $Zn_{48}S_{48}$,

and $Zn_{48}Se_{48}$ clusters show almost similar nature. For all the clusters, the HOMO is triply degenerate. The $Zn_{48}O_{48}$ spectra show more delocalized nature as compared to that of $Zn_{48}S_{48}$ and $Zn_{48}Se_{48}$. The delocalization of energy levels in $Zn_{48}O_{48}$ reflects higher degree of hybridization between Zn-O as compared to that of $Zn_{48}S_{48}$ and $Zn_{48}Se_{48}$ clusters. HOMO-LUMO gap of $Zn_{48}S_{48}$ is 2.94 eV and $Zn_{48}Se_{48}$ is 2.49 eV. These results are in agreement with earlier studies [6,15,17]. The calculated binding energies and HOMO-LUMO gap shows similar trend. The binding energy and HOMO-LUMO gap decreases from $O \rightarrow S \rightarrow Se$ in $Zn_{48}X_{48}$ cluster. As discussed earlier, the bonding between $Zn_{48}O_{48}$ cluster is dominant with ionic character.

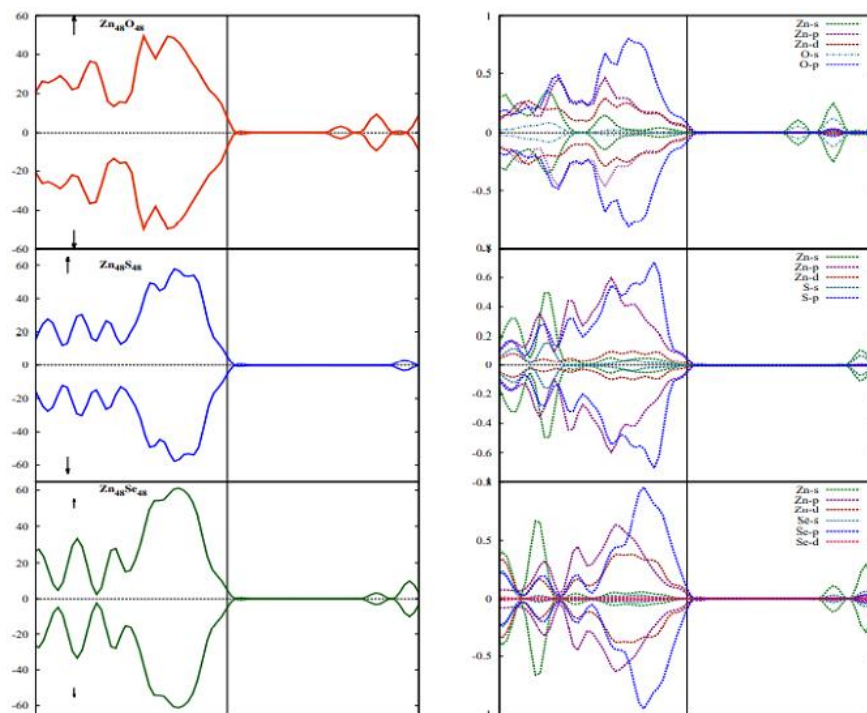


Figure 1.3: Total Density of States and Projected Density of States for $Zn_{48}X_{48}$ clusters with $X = O, S, Se$, respectively

The localized charge density is evidently seen around O atoms. From the charge density plots as shown in Figure 3.4 of $Zn_{48}S_{48}$ and $Zn_{48}Se_{48}$ cluster, it is also seen that the charge density associated with oxygens is polarized towards Zn atom. This indicated that $Zn_{48}S_{48}$ and $Zn_{48}Se_{48}$ are less ionic as compared to that of $Zn_{48}O_{48}$ cluster. It is clear from the lowering of maximum value of charge density value from $1/7^{th} \rightarrow 1/17^{th} \rightarrow 1/23^{th}$ from $O \rightarrow S \rightarrow Se$. To focus on the bonding nature further we have calculated charge transfer from Zn to O, S and Se atoms respectively using Bader charge analysis [13]. For $Zn_{48}O_{48}$ cluster, average charge transfer from $Zn(+1.07e)$ atom to $O(-1.07e)$ atom.

This shows ionic nature of Zn-O bond. Similarly, for $Zn_{48}S_{48}$ cluster, average charge transfer from $Zn(+0.84e)$ to $S(-0.84e)$ and in $Zn_{48}Se_{48}$ cluster, average charge transfer from $Zn(+0.68e)$ to $Se(-0.68e)$. Overall, all the clusters are showing ionic character but the charge transfer from $Zn \rightarrow O, Zn \rightarrow S$ and $Zn \rightarrow Se$ decreases from $O \rightarrow S \rightarrow Se$. The ionicity decreases from $Zn_{48}O_{48}$ to $Zn_{48}S_{48}$ to $Zn_{48}Se_{48}$. The decrease in charge transfer and ionicity is also reflected in total density of states of these clusters. Figure 3.5 represents, DOS and PDOS of $Zn_{48}X_{48}$ clusters. From the total density of states, it is seen that for $Zn_{48}O_{48}$ cluster the spectra are more delocalized as compared to that of $Zn_{48}S_{48}$ and $Zn_{48}Se_{48}$. This reflects the decrease in Zn-X hybridization from $O \rightarrow S \rightarrow Se$. From the projected density of states is found that the states near HOMO are clearly due to nonbonding (O/S/Se)-p states. The number of nonbonding states increases from $O \rightarrow S \rightarrow Se$. This observation is consistent with Bader charge analysis. The charge transfer from Zn decreases from $O \rightarrow S \rightarrow Se$. In the middle of the spectra the localized states of Zn-sd and X-p are observed in $Zn_{48}S_{48}$ and $Zn_{48}Se_{48}$. Next, we have studied optical properties of $Zn_{48}O_{48}$ cluster. We have calculated the imaginary and real part of dielectric function of

Zn₄₈O₄₈ along x, y, z direction. The imaginary and real parts of the dielectric values are plotted for all photon energies. The spectra isotropic in all x, y, z direction. Here, we have presented imaginary and real part along x direction over all photon energy in Figure 3.6.

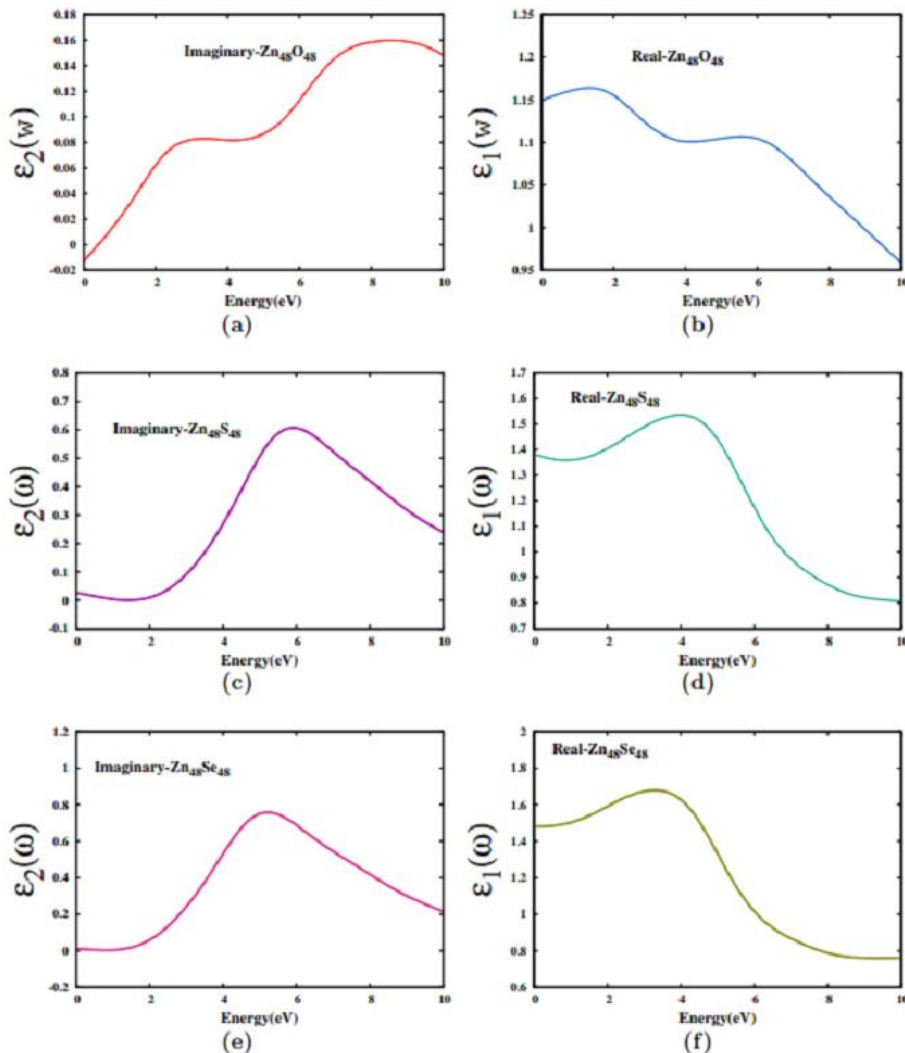


Figure 1.4: Optical plots of Zn₄₈X₄₈ clusters with X = O, S, Se, respectively. (a) Represents Imaginary part of optical spectra corresponding to Zn₄₈O₄₈ cluster. (b) Represents Real part of optical spectra corresponding to Zn₄₈O₄₈ cluster. (c) Represents Imaginary part of optical spectra corresponding to Zn₄₈S₄₈ cluster. (d) Represents Real part of optical spectra corresponding to Zn₄₈S₄₈ cluster. (e) Represents Imaginary part of optical spectra corresponding to Zn₄₈Se₄₈ cluster. (f) Represents Real part of optical spectra corresponding to Zn₄₈Se₄₈ cluster.

The imaginary part of $\sigma(\omega)$ is computed from $\text{Re } \sigma D(\omega)$ via the Kramers-Kronig relation. From the optical spectra, it is noted that all the clusters are transparent in visible region, with significant difference in Zn₄₈S₄₈ and Zn₄₈Se₄₈ clusters with high transparency in ultraviolet region. Imaginary peaks of Zn₄₈S₄₈ and Zn₄₈Se₄₈ shifted to higher energy values. The spectra for ZnS and ZnSe cluster shows blue shift as compared to ZnO cluster. Few transitions are actually forbidden in HOMO-LUMO gap. Hence, dominant peaks are considered those occurs due to transition from HOMO-LUMO. HOMO-LUMO gap of Zn₄₈S₄₈ is more than Zn₄₈Se₄₈ and Zn₄₈O₄₈. Thus, absorption peak of zinc sulphide cluster is at higher energy value, thus blue shift as compared to zinc oxide and zinc selenide clusters. The frequency dependent

real part of dielectric function provides the dielectric constant of these clusters. For $Zn_{48}O_{48}$ cluster dielectric constant is 1.14, $Zn_{48}S_{48}$ 1.49 and $Zn_{48}Se_{48}$ 1.62. From O to S to Se, the dielectric constant decrease for $Zn_{48}O_{48}$ cluster. This trend is consistent with increase in HOMO-LUMO gap of $Zn_{48}X_{48}$ cluster with $X = O, S, Se$. The increase in dielectric constant from $O \rightarrow S \rightarrow Se$ reflects the increase in conductivity of these clusters from $O \rightarrow S \rightarrow Se$.

IV. CONCLUSION

Based on the literature survey we have considered $Zn_{48}O_{48}$, $Zn_{48}S_{48}$ and $Zn_{48}Se_{48}$ clusters as a shell model. All these clusters are globular clusters with Th symmetry. The $Zn_{48}X_{48}$ clusters with $X = O, S, Se$ are nonmagnetic in nature. With the variation in $Zn_{48}X_{48}$ from $O \rightarrow S \rightarrow Se$, the HOMO-LUMO gap changes significantly which reflect the reactivity of shell material. It is found that among these three clusters, $Zn_{48}O_{48}$ is most stable as compared to that of $Zn_{48}S_{48}$ and $Zn_{48}Se_{48}$ cluster.

FUTURE SCOPE

Cage Clusters are having sufficient diameter to occupy small magnetic cluster. Nonmagnetic nature of these clusters is useful so as core-shell combination cluster should retain magnetic properties of core material. Optical properties of these clusters show transparency in visible region.

ACKNOWLEDGEMENTS

All authors would like to acknowledge CDAC Pune for providing supercomputing facility. DSL would like to express her sincere thanks to Dr. M. D. Deshpande Madam and H.P.T. Arts and R.Y.K. Science College, Nashik.

REFERENCES

- [1]. V. Kumar, K. Esfarjani, and Y. Kawazone. Springer Series in Cluster Physics Springer-Verlag, 2002.
- [2]. J. A. Alonso. Chem. Rev., 100:637, 2000.
- [3]. R. Ghosh Chaudhari and S. Paria. Chem. Rev., 112:2373, 2012.
- [4]. Hsueh-Shih Chen, Bertrand Lo, Jen-Yu Hwang, Gwo-Yang Chang, ChienMing Chen, and Shih-Jung Tasi. J. Phys. Chem. B., 108:17119, 2004
- [5]. Said Hamad, Scott M. Woodely, and C. Richard A. Catlow. Molecular Simulation, 35:1015, 2009.
- [6]. L. Ovsianikova. Phys. Solid State, 61:673, 2019.
- [7]. N. Cho, T. Cheong, J. HyunMin, J. HuaWu, S. Lee, D. Kim, J. Yang, S. Kim, Y. Kim, and S. Seong. Nature Nanotech., 6:675, 2011.
- [8]. Y. Hu, C. Ji, X. Wang, J. Huo, Q. Liu, and Y. Song. Scient. Rep., 7:16485, 2017.
- [9]. Vienna. ab initio Simulation Package (VASP), Technische Universitat Wien, 1999.
- [10]. G. Kresse and J. Furthmuller. Comput. Mater. Sci., 6:15, 1996.
- [11]. G. Kresse and D. Joubert. Phys. Rev. B, 59:1758, 1999.
- [12]. P. Bloch. Phys. Rev. B, 50:17953, 1994.
- [13]. W. Tang, E. Sanville, and G. Henkelman. J. Phys. Cond. Mat., 21:084204, 2009.
- [14]. B. Wang, X. Wang, G. Chen, S. Nagase, and J. Zhao. J. Chem. Phys., 128:144710, 2008.
- [15]. X. Wang B. Wang, G. Chen, S. Nagase, and J. Zhao. J. Chem. Phys., 12:144710, 2008.
- [16]. Klinton Davis, Ryan Yarbrough, Michael Froeschle, Jammel White, and Hemali Rathnayake. RSC Adv., 9:14638, 2019.
- [17]. L. Ovsianikova. Acta Physica Pollonica A, 122:1062, 2012.